COMMUNICATIONS

Population and coherence control by three-pulse four-wave mixing

Emily J. Brown, Igor Pastirk,[a] Bruna I. Grimberg, Vadim V. Lozovoy,[b] and Marcos Dantus[c]
Department of Chemistry and Center for Fundamental Materials Research, Michigan State University, East Lansing, Michigan 48824

(Received 28 April 1999; accepted 22 June 1999)

Control of coherence and population transfer between the ground and excited states is reported using three-pulse four-wave mixing. The inherent vibrational dynamics of the system are utilized in timing the pulse sequence that controls the excitation process. A slight alteration in the pulse sequence timing causes a change in the observed signal from coherent vibration in the ground state to coherent vibration in the excited state. This control is demonstrated experimentally for molecular iodine. The theoretical basis for these experiments is discussed in terms of the density matrix for a multilevel system. © *1999 American Institute of Physics.* [S0021-9606(99)03233-X]

The probability of exciting a molecular system from the ground, $|g\rangle$, to the excited state, $|e\rangle$, by applying an electric field $\mathbf{E}$ is written quantum mechanically as

$$P_{eg}=|\langle e|\boldsymbol{\mu}\cdot\mathbf{E}|g\rangle|^2=\langle e|\boldsymbol{\mu}\cdot\mathbf{E}|g\rangle\langle g|\boldsymbol{\mu}\cdot\mathbf{E}^*|e\rangle, \tag{1}$$

where μ is the transition dipole moment that couples both states. Population inversion is not usually achieved because of the competition between the rates of absorption and stimulated emission. Control of the population transfer can be achieved if the two electric fields involved in the transition probability in Eq. (1) are different and are correlated in time or in phase. The three-pulse four-wave mixing (FWM) technique allows one to combine three nonphase-locked electric fields in a phase-matching geometry. The first two fields cause the population transfer and the third field probes the system. The specific timing between the pulses can be used to control the values of diagonal (population) and off-diagonal (vibrational coherence) matrix elements after the interaction with the first two electric fields. In this Communication, we briefly describe the three-pulse FWM technique and demonstrate on molecular iodine that pulse sequences can be designed to control the transition probability between two electronic states of a molecule.

It has long been recognized that in order to optimize the transfer of population between two states sophisticated electric fields are required.[1–4] One can create such electric fields by a combination of phase and amplitude masks,[5–7] or one can combine phase-locked laser pulses to achieve the desired field. Scherer *et al.*[8] showed that when two phase-locked laser pulses were combined in phase the excited state dynamics of molecular iodine could be observed as fluorescence enhancement; however, when they were combined out of phase, the signal is observed as fluorescence depletion. Coherent control of chemical reactions depends on the relative phase of two different laser pulses that interact with the sample. The relative phase of the pulses can be used to control the population transfer from the ground to two different excited states.[9–11] A different approach to controlling population transfer[12] and enhancing reaction yields[13,14] uses chirped laser pulses. Recent experiments in our group using chirped femtosecond three-pulse FWM have demonstrated that laser chirp can be used to control coherence transfer between the ground and excited states of I_2.[15]

The theoretical foundation for three-pulse FWM is based on the time evolution of the density matrix in Hilbert space.[16] Formulas are derived for a multilevel system with ground and excited electronic states with vibrational levels. Ultrafast transform-limited pulses are assumed with a bandwidth that exceeds the vibrational spacing in the ground and excited states. Electric field interactions are treated within the perturbation limit. A more detailed description of this theory will be published elsewhere.[17,18] Initially, the density matrix, $\rho^{(0)}$, contains the populations of the vibrational levels of the ground state with $\Sigma\rho_{gg}^{(0)}=1$, while the population of each vibrational level in the excited state is taken as $\rho_{ee}^{(0)}=0$. Here, the index g corresponds to the ground state vibrational quantum number, ν'', and the index e corresponds to the excited state vibrational quantum number ν'. In our calculation, we assume that the ground state vibrational levels are equally populated. This assumption is justified for a high temperature Boltzmann distribution. Different initial vibrational population distributions yield similar results.[15,17] After the first interaction with the electric field, the density matrix evolves into a coherence between the ground and excited states where all the diagonal terms are zero and no net population transfer has occurred. The interaction with a second electric field completes the population transfer [Eq. (1)] without electronic coherence between the $|g\rangle$ and $|e\rangle$ states.

[a]Affiliated with the Institute for Nuclear Sciences ''VINCA,'' Belgrade, F. R. Yugoslavia.
[b]Permanent address: N. N. Semenov Institute of Chemical Physics, RAS, Moscow, Russia.
[c]Author to whom correspondence should be addressed; electronic mail: dantus@cem.msu.edu

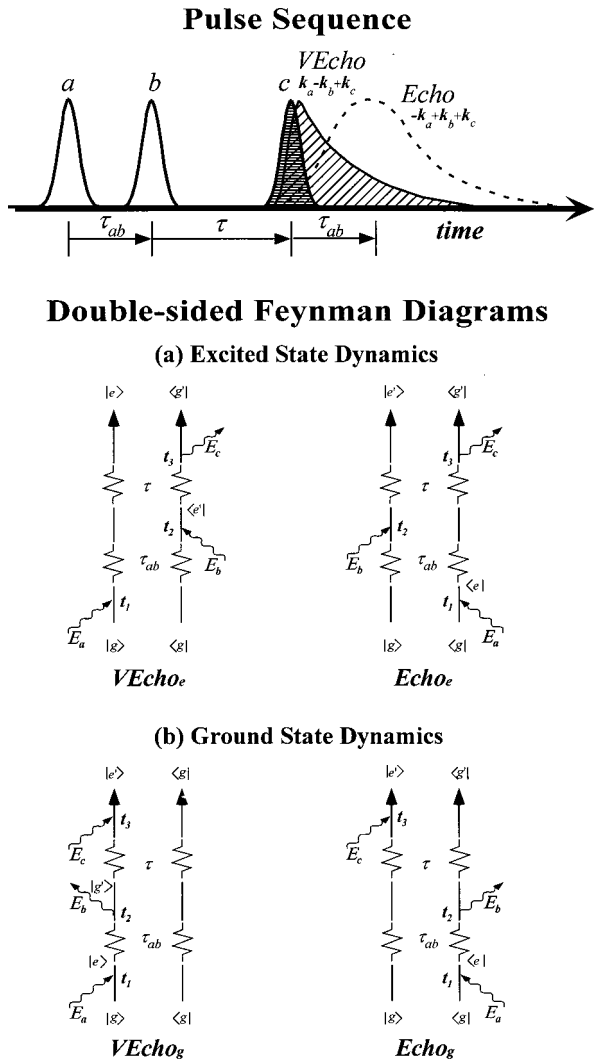

FIG. 1. Pulse sequence and double-sided Feynman diagrams corresponding to the three-pulse FWM measurements. The diagrams show the observation of (a) excited state dynamics and (b) ground state dynamics. In this pulse sequence, the first two electric fields are separated in time by τ_{ab}. The third beam is scanned in time with time delay τ. The diagrams on the left correspond to the virtual echo signal in the direction $\mathbf{k}_s=\mathbf{k}_a-\mathbf{k}_b+\mathbf{k}_c$; the diagrams on the right correspond to the echo signal in the direction $\mathbf{k}_s=-\mathbf{k}_a+\mathbf{k}_b+\mathbf{k}_c$. In our experimental setup, we detect signal only in the $\mathbf{k}_a-\mathbf{k}_b+\mathbf{k}_c$ direction.

In general, an odd number of interactions with the electric fields will produce a coherence state, which is also a time-dependent polarization of the molecules. An even number of interactions will produce a population state that is characterized by the population of the vibrational levels in each electronic state (the diagonal terms) and the vibrational coherence within each electronic state (the off-diagonal terms in the diagonal blocks).

The changes in the density matrix after each interaction with an electric field involve different processes that can be followed using double-sided Feynman diagrams.[16,19] For further information about these diagrams and their applications to four-wave mixing processes, the reader is referred to Refs. 16, 17, and 19–21. A wavy arrow symbolizes each electric field interaction and time progresses from the bottom to the top. The arrows pointing towards (away from) the center represent the photon annihilation (creation) operator; absorption or emission of a photon requires two electric field interactions. The diagrams in Fig. 1(a) show absorption of a photon and transfer of population to the excited state, while the diagrams in Fig. 1(b) show that the population remains in the ground state. The third pulse forms a polarization which emits radiation in the phase-matching direction $\mathbf{k}_s=\mathbf{k}_a-\mathbf{k}_b+\mathbf{k}_c$ or $\mathbf{k}_s=-\mathbf{k}_a+\mathbf{k}_b+\mathbf{k}_c$. The density matrix of the system depends on the sum of all the processes described by the four diagrams in Fig. 1. For calculating the density matrix (population and coherence) after two pulses, all diagrams must be used. Because we detect in the $\mathbf{k}_a-\mathbf{k}_b+\mathbf{k}_c$ direction, only the virtual echo processes are needed for calculating the emitted light after the third pulse. Furthermore, by proper selection of τ_{ab}, the time delay between the first two electric fields, we obtain a signal predominately from the excited or the ground state (i.e., ***VEcho***$_e$ or ***VEcho***$_g$).

The density matrix elements after two electric field interactions contain a dependence on τ_{ab} and this parameter can be used to control the transition probability from the ground to the excited state. After the second pulse is applied, the population transfer between the ground and excited states is given by

$$\sum_e \rho_{ee}^{(2)}-\sum_g \rho_{gg}^{(2)} \propto \cos\left(\frac{\omega_e\tau_{ab}}{2}\right)\cos\left(\frac{\omega_g\tau_{ab}}{2}\right)\cos(\omega\tau_{ab}-(\mathbf{k}_a-\mathbf{k}_b)\mathbf{r}), \quad (2)$$

where ω_g and ω_e are the vibrational frequencies of the ground and excited states, respectively, ω is the laser carrier frequency, and $\mathbf{r}$ is the spatial coordinate in the sample. After the third pulse is applied at time $\tau_{ab}+\tau$, the signal is a sum of two contributions, one from molecules that remained in the ground state following two interactions with the electric fields,

$$S_g \propto \sum_{\substack{g,g' \\ g\neq g'}} |\tilde{\rho}_{gg}^{(2)}-\tilde{\rho}_{g'g}^{(2)}|^2 \propto (1+\cos(\omega_e\tau_{ab}))(1+\cos(\omega_g\tau)), \quad (3a)$$

and the other from molecules in the excited state,

$$S_e \propto \sum_{\substack{e,e' \\ e\neq e'}} |\tilde{\rho}_{ee}^{(2)}+\tilde{\rho}_{ee'}^{(2)}|^2 \propto (1+\cos(\omega_g\tau_{ab}))(1+\cos(\omega_e\tau)), \quad (3b)$$

where $\tilde{\rho}^{(2)}$ indicates only the terms of $\rho^{(2)}$ that satisfy the phase-matching condition $\mathbf{k}_a-\mathbf{k}_b+\mathbf{k}_c$. The matrix elements $\rho_{g'g}^{(2)}$ and $\rho_{ee'}^{(2)}$ describe the vibrational coherence in the ground and the excited states, respectively. Note that the signal amplitude depends on both the population and coherence elements as seen in Eqs. (3). If we define $\tau_e=2\pi/\omega_e$ (and $\tau_g=2\pi/\omega_g$), at a time delay $\tau_{ab}=\tau_e(n+1/2)$, the signal for the ground state goes to zero. When $\tau_{ab}=\tau_e n$, the signal for the ground state reaches a maximum. Similarly $\tau_{ab}=\tau_g(n+1/2)$ and $\tau_{ab}=\tau_g n$ correspond to the minimum and maximum signals from the excited state, respectively. Maximum control can be achieved for values of τ_{ab} that maximize one

contribution and, at the same time, minimize the other. These values can always be found provided $\omega_g \neq \omega_e$. The definition of a single vibrational frequency for each electronic state is applicable for a four-level system with two vibrational levels in each state. Extension of these formulas beyond four levels would require the introduction of anharmonicity. The four-level model used here successfully predicts the observed experimental results (*vide infra*).

The experimental setup used to carry out the measurements has been described elsewhere.[21] Briefly, transform-limited pulses with a 60 fs temporal width [full width at half maximum (FWHM)] and with the central wavelength at 620 nm were used in these measurements. The laser beam was split and the three beams were combined in the forward box geometry. The energy per pulse for each beam was $\sim 20\ \mu$J. The pulses were focused into a quartz cell containing neat iodine vapor at 140 °C. The three-pulse FWM signal was collected by a spectrometer with a very broad spectral acceptance (16 nm). Spectrally dispersed three-pulse FWM measurements will be published elsewhere.[15]

The two transients shown in Fig. 2 were collected consecutively under identical conditions. The only difference between them was the time delay (τ_{ab}) between the first two pulses. Based on the theory, various multiples of the ground or excited state vibrational periods can be used to achieve control over the population transfer.[17] We have tried a number of combinations with great success. We have chosen to use 460 fs ($\frac{3}{2}\tau_e$) and 614 fs ($2\tau_e$) which correspond to times when the ground state population is at a minimum and a maximum, respectively. The transients are the result of 20 scans containing 200 different time delays between the second and third pulses (τ).

For experiments with $\tau_{ab}=0$ fs, a setup that is also known as a transient grating, the transients (not shown here) contain both ground and excited state vibrational dynamics.[17,21,22] Figure 2(a) shows the three-pulse FWM signal obtained with $\tau_{ab}=460\pm10$ fs. The transient shows vibrational oscillations with a period of 307 fs corresponding to dynamics in the B $^3\Pi_{o+u}$ state involving vibrational levels $v'=6-11$. The power fast Fourier transform (FFT) of the transient is shown in Fig. 2(c) (black line). The most prominent peak is centered at $107.7\pm0.2\ \mathrm{cm}^{-1}$ and corresponds to the excited state dynamics. A small peak centered at $218.2\pm0.2\ \mathrm{cm}^{-1}$ is the second harmonic of the excited state signal and is not a contribution from the ground state. The small peak centered at $10.8\pm0.5\ \mathrm{cm}^{-1}$ corresponds to the rotational dephasing dynamics.[21]

Figure 2(b) shows the three-pulse FWM signal obtained for $\tau_{ab}=614\pm10$ fs. The transient shows vibrational oscillations with a period of 160 fs corresponding to dynamics in the $X\ ^1\Sigma_{0+g}$ state involving vibrational levels $v''=3,4$. The power FFT of the transient is shown in Fig. 2(c) (gray line). The most prominent peak is centered at $208.3\pm0.1\ \mathrm{cm}^{-1}$ and corresponds to ground state vibrational dynamics. A smaller peak centered at $107.1\pm0.1\ \mathrm{cm}^{-1}$ corresponds to a minor contribution from the excited state which is expected for this value of τ_{ab} [see Eqs. (3)]. The small peak centered at $15.9\pm0.4\ \mathrm{cm}^{-1}$ corresponds to the rotational dephasing dynamics. The rotational constants for the ground and excited states differ by a factor of 1.34;[23,24] the ratio of the observed frequencies due to rotations is 1.47 ± 0.11.

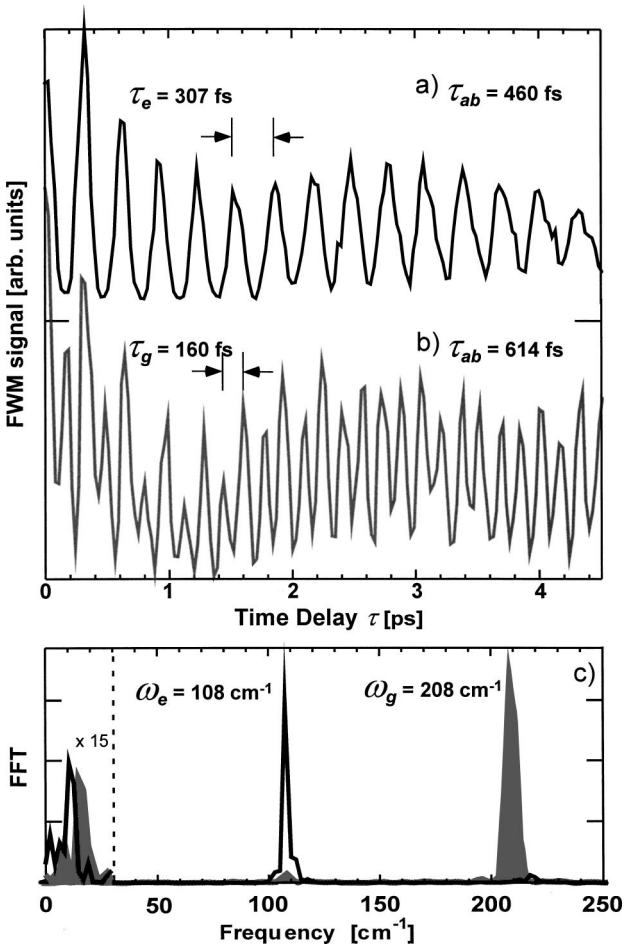

FIG. 2. Experimental demonstration of population control using three-pulse FWM. (a) Transient showing excited state vibrational dynamics with a period of 307 fs. (b) Transient showing ground state vibrational dynamics with a period of 160 fs. Note that these transients have been displaced vertically by 1 tick mark. (c) Power FFT corresponding to each transient. For the FFT of the first transient (black line), the most prominent peak is centered at $107.7\pm0.2\ \mathrm{cm}^{-1}$ corresponding to the vibrational dynamics of iodine in the excited state. The small peak centered at $218.2\pm0.2\ \mathrm{cm}^{-1}$ is the second harmonic of the excited state vibrational frequency. The peak centered at $10.8\pm0.5\ \mathrm{cm}^{-1}$ corresponds to the rotational motion of the ground state. For the FFT of the second transient (gray line), the most prominent peak is centered at $208.3\pm0.1\ \mathrm{cm}^{-1}$ corresponding to the vibrational dynamics of iodine in the ground state. There is a small peak centered at $107.1\pm0.1\ \mathrm{cm}^{-1}$ indicating some contribution from the excited state. The peak centered at $15.9\pm0.4\ \mathrm{cm}^{-1}$ corresponds to the rotational motion. Note that the data in the range of $0-30\ \mathrm{cm}^{-1}$ are magnified 15 times.

The experimental data presented here show that the time delay between the first two pulses in a three-pulse FWM experiment can be used to control the population transfer between ground and excited states. We have used this technique in order to study the vibrational dephasing in the ground and excited states of iodine as a function of temperature and pressure. By changing τ_{ab} we were able to obtain both separate values from the same setup.[25] The ability to transfer populations between different states is the chief tenet of the pump-dump control theory of Rice and Tannor.[26,27] With three-pulse FWM we have shown that this control can be achieved with great efficiency. This technique can be use-

ful to study ultrafast dynamics involved in chemical reactions where one may want to follow processes that occur in the excited or the ground state exclusively.

Experimental control using multiple laser pulse excitation has been explored by a number of groups.[1] While some of these experiments have been carried out without phase-locked pulses or phase-matching conditions,[28–30] the most striking control over the excitation process is observed for phase-matched or phase-locked setups. Scherer *et al.* measured this effect by observing a change in the total fluorescence of I_2.[8] Warren and Zewail used collinear phase-locked pulses to observe photon echos in I_2.[31] Pshenichnikov *et al.* used a phase-locked FWM arrangement where the virtual echo and conventional echo processes interfere constructively or destructively.[32] Time-delayed pulses can be combined to achieve population inversion by adiabatic passage.[33,34] From Eq. (2), one can see that the population transfer is modulated by an electronic term with control parameter $\omega\tau_{ab}$ and a spatial condition $(\mathbf{k}_a-\mathbf{k}_b)\mathbf{r}$. The amplitude is further governed by the vibrational motion of both electronic states with control parameters $\omega_e\tau_{ab}$ and $\omega_g\tau_{ab}$. Our measurements use the vibrational time scale, which is independent of phase locking, to achieve the control.

In summary, we have demonstrated that pulse sequences can be found for three-pulse FWM experiments to optimize population and coherence transfer between two electronic states. In particular, we showed that the ground state population, after the first two pulses, could be controlled using a time that depends on the period of the excited state vibrational dynamics. We showed that for $\tau_{ab}=460$ fs only excited state dynamics are observed, while for $\tau_{ab}=614$ fs primarily ground state dynamics are observed. We plan to expand these types of experiments to systems where it will be possible to control the outcome of chemical reactions.

This article is dedicated to Professor Kent R. Wilson. His contributions to laser control of chemical reactions have energized and inspired a large number of researchers. This research was partially funded by a grant from the National Science Foundation (CHE-9812584). One of the authors (M.D.) is a Lucille and David Packard Science and Engineering fellow, a Camille Dreyfus Teacher-Scholar, and an Alfred P. Sloan fellow. The authors want to thank Professor Shaul Mukamel for insightful comments. One author (E.J.B.) was supported by a National Science Foundation Graduate Fellowship.

[1] R. J. Gordon and S. A. Rice, Annu. Rev. Phys. Chem. **48**, 601 (1997).
[2] R. S. Judson and H. Rabitz, Phys. Rev. Lett. **68**, 1500 (1992).
[3] A. Assion, T. Baumert, M. Bergt, T. Brixner, B. Kiefer, V. Seyfried, M. Strehle, and G. Gerber, Science **282**, 919 (1998).
[4] J. S. Cao, C. J. Bardeen, and K. R. Wilson, Phys. Rev. Lett. **80**, 1406 (1998).
[5] C. W. Hillegas, J. X. Tull, D. Goswami, D. Strickland, and W. S. Warren, Opt. Lett. **19**, 737 (1994).
[6] M. M. Wefers and K. A. Nelson, Opt. Lett. **20**, 1047 (1995).
[7] A. M. Weiner, Prog. Quantum Electron. **19**, 161 (1995).
[8] N. F. Scherer, A. J. Ruggiero, M. Du, and G. R. Fleming, J. Chem. Phys. **93**, 856 (1990).
[9] P. Brumer and M. Shapiro, Acc. Chem. Res. **22**, 407 (1989).
[10] C. Chen, Y.-Y. Yin, and D. S. Elliot, Phys. Rev. Lett. **64**, 507 (1990).
[11] L. C. Zhu, V. Kleiman, X. N. Li, S. P. Lu, K. Trentelman, and R. J. Gordon, Science **270**, 77 (1995).
[12] V. Yakovlev, C. J. Bardeen, J. Che, J. Cao, and K. R. Wilson, J. Chem. Phys. **108**, 2309 (1998).
[13] C. J. Bardeen, J. W. Che, K. R. Wilson, V. V. Yakovlev, P. J. Cong, B. Kohler, J. L. Krause, and M. Messina, J. Phys. Chem. A **101**, 3815 (1997).
[14] I. Pastirk, E. J. Brown, Q. Zhang, and M. Dantus, J. Chem. Phys. **108**, 4375 (1998).
[15] I. Pastirk, V. V. Lozovoy, B. I. Grimberg, E. J. Brown, and M. Dantus, J. Phys. Chem. A (submitted).
[16] S. Mukamel, *Principles of Nonlinear Optical Spectroscopy* (Oxford, New York, 1995).
[17] I. Pastirk, E. J. Brown, B. I. Grimberg, V. V. Lozovoy, and M. Dantus, Faraday Discuss. (to be published).
[18] B. I. Grimberg, V. V. Lozovoy, and M. Dantus (in preparation).
[19] Y. R. Shen, *The Principle of Nonlinear Optics* (Wiley, New York, 1984).
[20] P. H. Vaccaro, in *Nonlinear Spectroscopy for Molecular Structure Determination*, edited by E. Hirota, R. W. Field, J. P. Maier, and S. Tsuchiya (Blackwell Scientific, London, 1997).
[21] E. J. Brown, Q. Zhang, and M. Dantus, J. Chem. Phys. **110**, 5772 (1999).
[22] M. Schmitt, G. Knopp, A. Materny, and W. Kiefer, Chem. Phys. Lett. **280**, 339 (1997).
[23] M. Gruebele, G. Roberts, M. Dantus, R. M. Bowman, and A. H. Zewail, Chem. Phys. Lett. **166**, 459 (1990).
[24] R. J. LeRoy, J. Chem. Phys. **52**, 2683 (1970).
[25] V. V. Lozovoy, I. Pastirk, and M. Dantus, J. Chem. Phys. (submitted).
[26] D. J. Tannor, R. Kosloff, and S. A. Rice, J. Chem. Phys. **85**, 5805 (1986).
[27] D. J. Tannor and S. A. Rice, Adv. Chem. Phys. **70**, 441 (1988).
[28] J. J. Gerdy, M. Dantus, R. M. Bowman, and A. H. Zewail, Chem. Phys. Lett. **171**, 1 (1990).
[29] J. L. Herek, A. Materny, and A. H. Zewail, Chem. Phys. Lett. **228**, 15 (1994).
[30] M. Motzkus, S. Pedersen, and A. H. Zewail, J. Phys. Chem. **100**, 5620 (1996).
[31] W. S. Warren and A. H. Zewail, J. Chem. Phys. **75**, 5956 (1981).
[32] M. S. Pshenichnikov, W. P. d. Boeij, and D. A. Wiersma, Phys. Rev. Lett. **76**, 4701 (1996).
[33] J. S. Melinger, A. Hariharan, S. R. Gandhi, and W. S. Warren, J. Chem. Phys. **95**, 2210 (1991).
[34] B. W. Shore, J. Martin, M. P. Fewell, and K. Bergmann, Phys. Rev. A **52**, 566 (1995).